Half-metallic ferromagnetism in double perovskite Ca_2CoMoO_6 compound: DFT+*U* calculations

A. Djefal[1], S. Amari[1,2], L. Beldi[1], H. Bendaoud[1], R. F. L. Evans[3] and B. Bouhafs[1,*]

[1]Laboratoire de Modélisation et Simulation en Sciences des Matériaux, Université Djillali Liabès de Sidi Bel-Abbès, Sidi Bel-Abbès, 22000, Algeria.

[2] Faculty of Nature and Life Science, Hassiba Benbouali University of Chlef, 02000, Algeria

[3]Department of Physics, University of York, York YO10 5DD, UK.

Abstract:

A systematic investigation on magnetism and spin-resolved electronic properties in double perovskite Ca_2CoMoO_6 compound was performed by using the full-potential augmented plane wave plus local orbitals (APW+*lo*) method, within the generalized gradient approximation (GGA-PBE) and GGA-PBE+*U* scheme. It is shown the stability of the monoclinic phase (P21/n #14) relative to tetragonal (I4/m#87) and cubic (Fm3m #225). We also investigate the effect of Hubbard parameter *U* on the ground-state structural parameters and electronic properties. The analysis of the calculated spin-polarized band structures and densities of states indicate that Ca_2CoMoO_6 compound was half-metallic (HM) and half-semiconductor (HSC) ferromagnetic (FM) semiconductor with a total magnetic moment of 6.0, when using GGA-PBE and GGA-PBE+*U*, respectively.

An estimation of exchange couplings and magnetic Curie temperature has been given using the Vampire code. Further, our results regarding to the magnetic properties of this compound reveal their ferromagnetic nature. The GGA-PBE+*U* approach provides better band gap results as compared to GGA-PBE approximation. These results imply that Ca_2CoMoO_6 could be a promising magnetic semiconductor for application in spintronic devices.

Keywords: Density functional theory; Spin-polarization; Half-metallicity; Electronic structure; Ferromagnetism; GGA-PBE+*U*; Ordered double-perovskite.

1. Introduction

In the last decade double perovskites $A_2BB`O_6$ (A: Alkali metal, alkaline earth metal or lanthanides ) with transition metals at the BB` sites have been extensively studied due to their interesting physical properties, metallicity, half-metallicity, insulating as well as ferromagnetism (FM), antiferromagnetism (AFM), ferrimagnetism (FIM), which make them attractive candidates for spintronic applications like (Sr_2FeMoO_6) Kobay [1], also materials for magneto-optic devices [2].

This class of materials can exhibit a variety of crystallographic structures for different alkaline and transition metal ions the structure can be in room temperature: cubic (*Fm*-3*m* #225) as for example Ba_2FeMoO_6 [3], tetragonal (*I*4/*m*) Sr_2CoWO_6 [4], monoclinic (*P*2*1*/*n* #14) Ca_2FeMoO_6 [5].

Among this family, a studies have been made in the compound Ca_2FeMoO_6 show ferromagnetism and metallic behavior with high curie temperature [5]. Recently, the double perovskites compounds $Ca_2Fe_{1-x}Co_xMoO_6$ ($0.1 \leq x \leq 0.4$) have been prepared using solid-state reaction technique [6], the study show that with the increasing of the Co concentration, the lattice volume increases keeping the crystal structure, also a reduction of metallicity with the increasing Co substitution. To the best of our knowledge, there are no previous detailed studies on the electronic and magnetic properties for Ca2CoMoO6.

In this paper, we carried out first-principles calculations to investigate the structure stability of Ca_2CoMoO_6 using both GGA-PBE and GGA-PBE+*U*. we show that the material crystallize in a monoclinic system (P21/n) also we shall review the electronic structure, and it is interesting to show the effect of the *U* (Coulomb interaction correction) on the magnetic behavior and the magnetic properties, finally we give approximation of the magnetic curie

temperature. The paper is organized as follows: In Section 2, we make a brief review of the theoretical method. The results and some discussion are presented in Section 3. Finally, the conclusions derived from our calculations are summarized in Section 4.

2. Computational details

Total energies of all crystal structures are computed using DFT within both the generalized gradient approximation (GGA-PBE) and (GGA-PBE+*U)* approaches where *U* is on site Coulomb interaction correction. The crystal structure and ionic position were optimized using full-potential augmented plane wave method (FP-LAPW) implemented in wien2k code [7]. In the FP-LAPW method the wave function and potential are expanded in spherical harmonic functions inside non-overlapping spheres surrounding the atomic sites (muffin-tin spheres). The Brillouin zone were sampled with a 10×10×7 k-point mesh and the $R_{MT}\times K_{MAX}$ is set to 8, the muffin-tin (MT) radii of calcium, cobalt, molybdenum and oxygen are set to 2.02, 2.04, 1.75 and 1.55, respectively. To study the electronic and magnetic properties of Ca_2CoMoO_6, the Hubbard parameter is set to 5 eV ,1 eV for the strongly correlated Co 3*d* electrons [6] and the weakly correlated Mo 4*d* electrons [8], respectively.

3. Results

a) Structural properties and Magnetic stability:

For the identification of the phase stability, we have given the total energy as a function of volume using GGA-PBE and GGA-PBE+*U* for these three phases, cubic (Fm3m #225), tetragonal (I4/m#87) and monoclinic (P21/n #14), as shown in **Fig. 1**. As seen in **Fig. 1**, the monoclinic phase (P21/n #14) is more stable. We carried out full structure optimization calculation for the double perovskite Ca_2CoMoO_6 compound, the bulk modulus, and its pressure derivative have been computed by means of Murnaghan's equation of states [7]

represented by GGA-PBE and GGA-PBE+*U* for the three phases are listed in **Table 1**.To the best of our knowledge, no experimental or ab initio data on the structural properties of are available in the literature. Hence, our results can serve as a prediction for future investigations. We have used both the GGA and GGA+*U* schemes as a comparison in our calculations.

The atomic positions relaxations of the monoclinic phase are given in **Table 2**. Unfortunately, there are no experimental or ab initio data for comparing with our results. The lattice constants obtained within GGA-PBE+*U* are slightly increased compared to those of the GGA-PBE calculation.

The monoclinic structure of double perovskite Ca_2CoMoO_6 is optimized for different magnetic spin configurations, namely, a ferromagnetic spin configuration (FM) and two independent anti-ferromagnetic spin configurations (AFM), AFM1 with both Co and Mo in the AFM coupling along the c axis, and AFM2 with Co and Mo in the AFM and FM coupling along the c axis, respectively, as shown in **Fig. 2.** For more details, we have given also the total energy as a function of volume for all configurations considering the monoclinic phase (P21/n #14) with ferromagnetic (FM), anti-ferromagnetic (AFM1 and AFM2) (**Fig. 3**) using GGA-PBE and GGA-PBE+*U*. The total energy with FM ordering is stable with a very slight difference between total energies for both AFM1 and AFM2 when using GGA-PBE, while the FM configuration becomes more stable also we mark energy deference between (AFM1 and AFM2) configurations when applying the *U* correction, from this figure the Ca_2CoMoO_6 exhibits a ferromagnetic behavior.

b) Electronic structure :

Firstable, we calculate the electronic band structure of the ground state with the ferromagnetic spin configuration within GGA-PBE. We find the system has an apparent half metallic nature. The majority spins bands exhibit a band gap of 2.03 eV, while the minority spins bands cross the Fermi level. **Fig. 4** shows the Co 3*d* states at the vicinity of the Fermi level. However these states are down below the Fermi level in the spin up channel. We have also performed the calculations by the GGA-PBE+*U* method in order to certify the half metallic nature and investigate the effect of *U* on the electronic properties with *U*=(5.0,1.0) for both Co and Mo respectively. **Fig. 5** shows the dispersion of bands in the energy range around the Fermi level with applied of *U.* We find the gap in the up-spin bands enlarges (2.589eV) while in down-spin bands it is easily seen that with the effect of *U*, the Co (3*d* down) states are pushed up keeping metallic, and the Co (3*d* up) states are pulled down.

Fig. 6.a presents the density of states of Ca_2CoMoO_6 in GGA-PBE calculations. The electronic structure has a mechanism of HM characteristics. Below the Fermi level (E_F), the O 2*p* orbital extends from about -6.5 eV to -1.2 eV and hybrids with the Co 3*d* orbitals which are in the same energy region. The Mo 4*d* orbitals present in the conduction band in the energy range 1.6-2.5 eV, the band gap appears at the spin-up channel. In the spin-down channel, the Co 3*d* states dominate at the Fermi level from -0.5-0.1 eV.

To further understand the electronic structure using GGA-PBE+*U* method as shown in **Fig. 6.b**, the valence band consists purely of Co 3*d* orbitals at the vicinity of the Fermi-level with the Mo 4*d*-O 2*p*- Co 3*d* hybridization at the spin down direction. However the compound Ca_2CoMoO_6 appeared to be half-metallic with total magnetic moments arising from mainly the magnetic moment of Co and a weak magnetic moment for Mo calculated within GGA-PBE, GGA-PBE+*U* (given in **Table 3**).

c) Exchange couplings and magnetic Curie temperature:

The Curie temperature of a magnetic material principally defined by the exchange interaction, which determines the alignment of atomic spins, and makes a material ferromagnetic on the macroscopic scale. Vampire software package [9] [12] [13] contains a predefined function to calculate the Curie temperature of a material by performing a temperature sweep and calculating the average magnetization, giving the classic (M-T) curve. The exchange energy is calculated from the expression

$$H = -\sum_{<ij>} j_{ij} S_i \cdot S_j$$

Where J_{ij} is the exchange energy between nearest neighboring spins, and S_i is spin operator at site i (in both of the Co and Mo sublattices), there exists a relation between the energies e_{ij} and constants J_{ij} which can be expressed and estimated as follows:

$e_{ij} = J_{ij}\, S_i .\, S_j$

Where Si takes either $\frac{3}{2}$ or $\frac{1}{2}$ to the Co and Mo spins, the exchange interactions were obtained by mapping abinitio electronic structure calculations to the classical Heisenberg Hamiltonian [10]. From total energy differences (relative to FM configuration), we obtain the following equations from the three magnetic structures by considering only the nearest-neighbor:

$$\begin{cases} 0 = 8e_{\text{Co-Mo}} + 3e_{\text{Co-Co}} + 3e_{\text{Mo-Mo}} \\ E_{\text{AFM1}} - E_{\text{FM}} = -e_{\text{Co-Co}} - e_{\text{Mo-Mo}} \\ E_{\text{AFM2}} - E_{\text{FM}} = -4e_{\text{Co-Mo}} - e_{\text{Co-Co}} \end{cases}$$

We solve the e_{ij} parameters from the above equation set, and then calculate J_{ij} by using the above relation in both GGA-PBE and GGA-PBE+U method. The spin exchange energies e_{ij} and constants J_{ij} are summarized in **Table 4**. We also define the atomic spin moment of both Co and Mo atoms (**Table 3**), the periodic boundary conditions in all three spatial dimensions

is set with respectively (L=10, 20 and 30 *nm*). The calculated T_C value is equivalent to 278 K shown in **Fig. 7**.

4.Conclusion

In summary, using the first-principles FP-LAPW method within GGA–PBE and GGA-PBE+U for the exchange correlation functional, we have investigated the electronic structure and ferromagnetism for Ca_2CoMoO_6. The band spin-polarized calculations to show that the Ca_2CoMoO_6 is a half-metallic ferromagnetic with the Mo 4*d*-O 2*p*-Co 3*d* hybridization. The total spin magnetic moment of this compound is 6 μ_B/cell, which mainly comes from Co atoms. Our results are useful to understanding such materials and exploring their potential applications in spintronic.

Acknowledgements

One of us (B. B.) acknowledges the Algerian Academy of Sciences and Technologies (AAST) and the Abdus-Salam International Center for Theoretical Physics (ICTP, Trieste, Italy).

Table Captions

Table 1: The calculated lattice constants (a, b, c in Å, and β), the bulk modulus B (in GPa) and its derivative (B') of the Ca_2CoMoO_6 perovskite in $P2_1/n$ monoclinic symmetry for FM ordering, obtained using GGA-PBE and GGA-PBE+U.

Table 2: The Wyckoff positions of the double perovskite Ca_2CoMoO_6 compound in the monoclinic structure.

Table 3: The calculated total magnetic moment μ_{tot} (in μ_B/Cell) per cell and the local magnetic moments μ_{Co}, μ_{Mo} (in μ_B/atom) of Co, and Mo atoms, respectively, the half metallic gap E_g^{HM} (in eV) and the half semiconductor gap E_g^{HSC} (in eV) using GGA-PBE and GGA-PBE+U, respectively.

Table 4: The calculated spin exchange energies e_{ij} and constants J_{ij} in (meV) of double perovskite Ca_2CoMoO_6 for the nearest-neighbor within GGA-PBE and GGA-PBE +U.

Figures Captions

Fig. 1: Total energy as a function of volume for the ferromagnetic (FM) spin orderings of Ca_2CoMoO_6 compound in the cubic, tetragonal, and monoclinic structures using (a) GGA-PBE and (b) GGA-PBE+*U*

Fig. 2: Drawings of crystal structures of the (a) ferromagnetic FM and the anti-ferromagnetic (b) AFM1, and (c) AFM2 spin configurations of Ca_2CoMoO_6 compound in the monoclinic structure produced by VESTA [11].

Fig. 3: Total energy as a function of volume for the ferromagnetic (FM) and anti-ferromagnetic, AFM1, and AFM2 spin orderings of the monoclinic Ca_2CoMoO_6 compound using (a) GGA-PBE and (b) GGA-PBE+*U*.

Fig. 4: The calculated spin-polarized band structures (*a*) spin up, and (*b*) spin down, at the equilibrium lattice constant of the monoclinic double perovskite Ca_2CoMoO_6 compound, using GGA-PBE. The horizontal dashed line indicates the Fermi level.

Fig. 5: The calculated spin-polarized band structures (*a*) spin up, and (*b*) spin down, at the equilibrium lattice constant of the monoclinic double perovskite Ca_2CoMoO_6 compound, using GGA-PBE+*U*. The horizontal dashed line indicates the Fermi level.

Fig. 6: The calculated spin-polarized total and partial DOS of the monoclinic double perovskite Ca_2CoMoO_6 compound using (a) GGA-PBE and (b) GGA-PBE+*U*. The vertical dashed line indicates the Fermi level. The positive and negative values of DOS, hold for spin-up and spin-down states, respectively.

Fig. 7: The temperature dependent magnetization of the monoclinic double perovskite Ca_2CoMoO_6 compound, calculated using the atomistic spin model simulations implemented in the Vampire software package [12] [13].

Table 1

		a	***b***	***c***	***β***	***B***	***B'***
Monoclinic ($P2_1/n$)	GGA-PBE	5.55	5.65	7.91	90.2	163	4.38
	GGA-PBE+U	5.56	5.65	7.92	90.2	162	4.45
Tetragonal ($I4/m$)	GGA-PBE	5.40	5.40	7.80		184	4.60
	GGA-PBE+U	5.45	5.45	7.88		178	4.45
Cubic (Fm-3m)	GGA-PBE	7.72	7.72	7.72		201	4.38
	GGA-PBE+U	7.75	7.75	7.75		184	4.52

Table 2

			Ca	**Co**	**Mo**	**O (1)**	**O (2)**	**O (3)**
		Site	4*e*	2*c*	2*d*	4*e*	4*e*	4*e*
Present work	GGA-PBE	*x*	0.0110	0.5	0	0.2842	0.3090	0.9116
		y	0.0531	0	0.5	0.3024	0.2797	0.4699
		z	0.2548	0	0	0.0422	0.4488	0.2382
	GGA-PBE+U	*x*	0.0119	0.5	0	0.2829	0.3135	0.9065
		y	0.0535	0	0.5	0.3070	0.2806	0.4664
		z	0.2543	0	0	0.0444	0.4452	0.2355

Table 3

	μ_{Total}	μ_{Co}	μ_{Mo}	E_g^{HM}	E_g^{HSC}
GGA-PBE	6	2.571	0.008	0.70	
GGA-PBE+U	6	2.760	0.017		0.93

Table 4

	e_{ij} **(meV)**		J_{ij} **(meV)**	
	GGA-PBE		GGA-PBE+U	
Co-Mo	7.42	9.90	6.89	9.19
Co-Co	-49.08	-21.81	-37.25	-16.55
Mo-Mo	29.27	117.1	18.87	75.47

Fig. 1

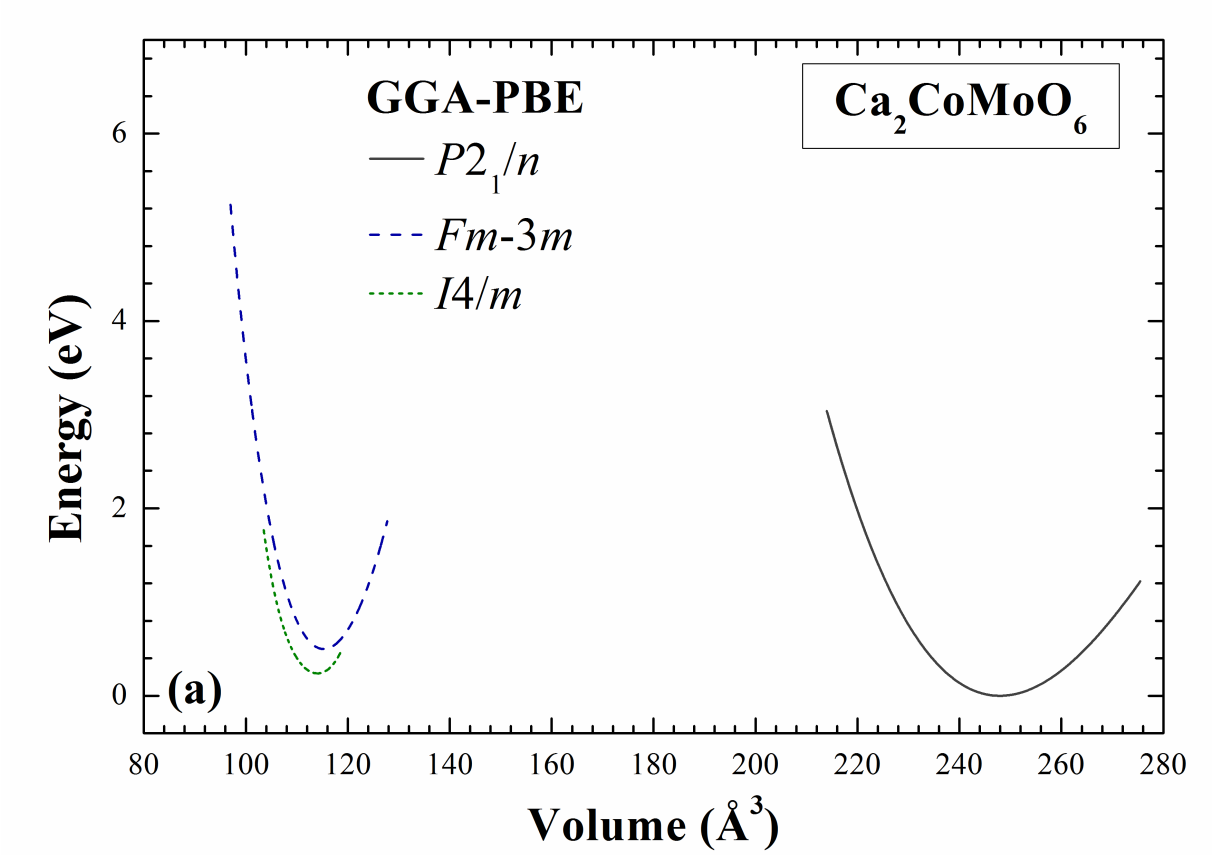
GGA-PBE
Ca2CoMoO6
P21/n
Fm-3m
I4/m
Energy (eV)
Volume (Å3)
(a)
0
2
4
6
80
100
120
140
160
180
200
220
240
260
280

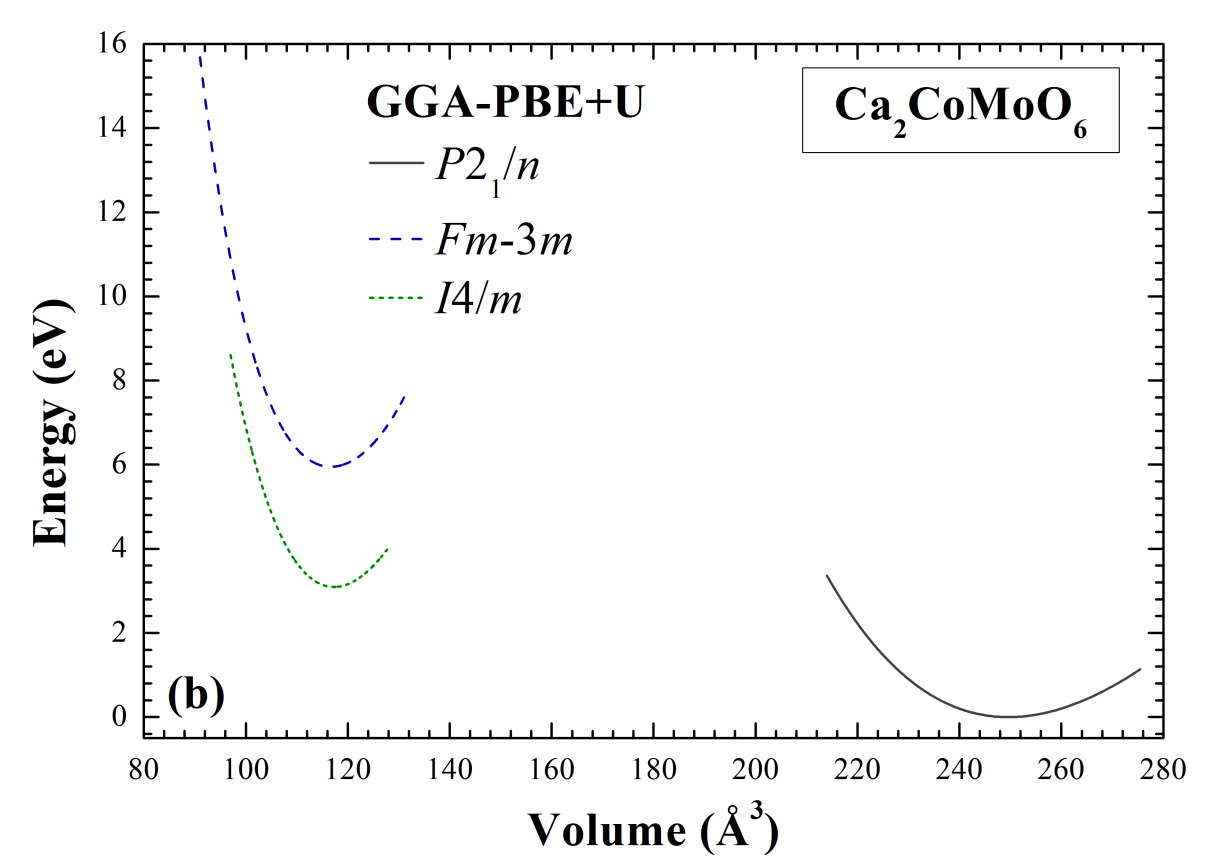
GGA-PBE+U
Ca2CoMoO6
P21/n
Fm-3m
I4/m
Energy (eV)
Volume (Å3)
(b)
0
2
4
6
8
10
12
14
16
80
100
120
140
160
180
200
220
240
260
280

Fig. 2

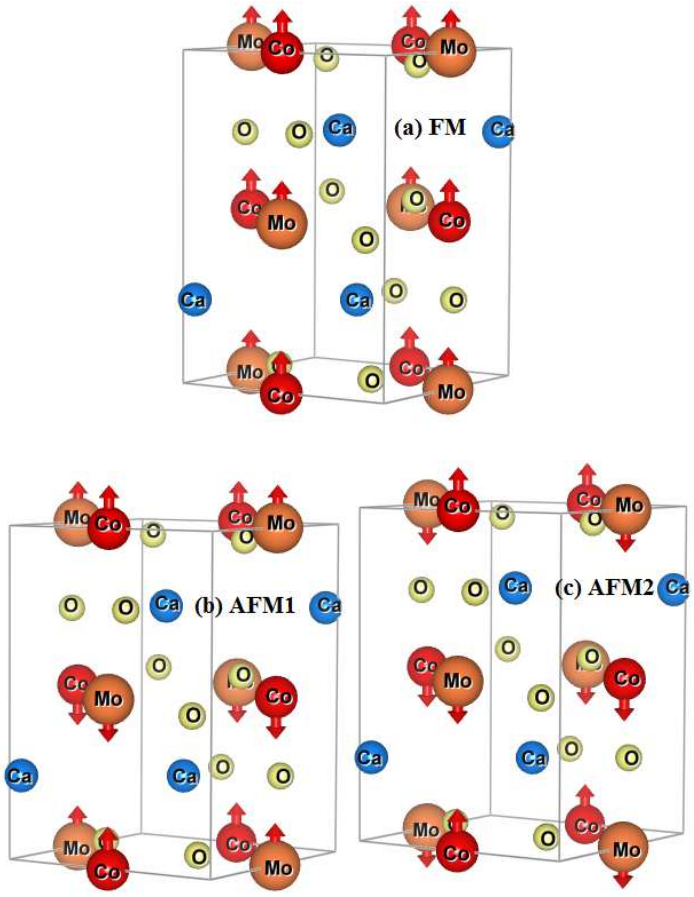

Fig. 3

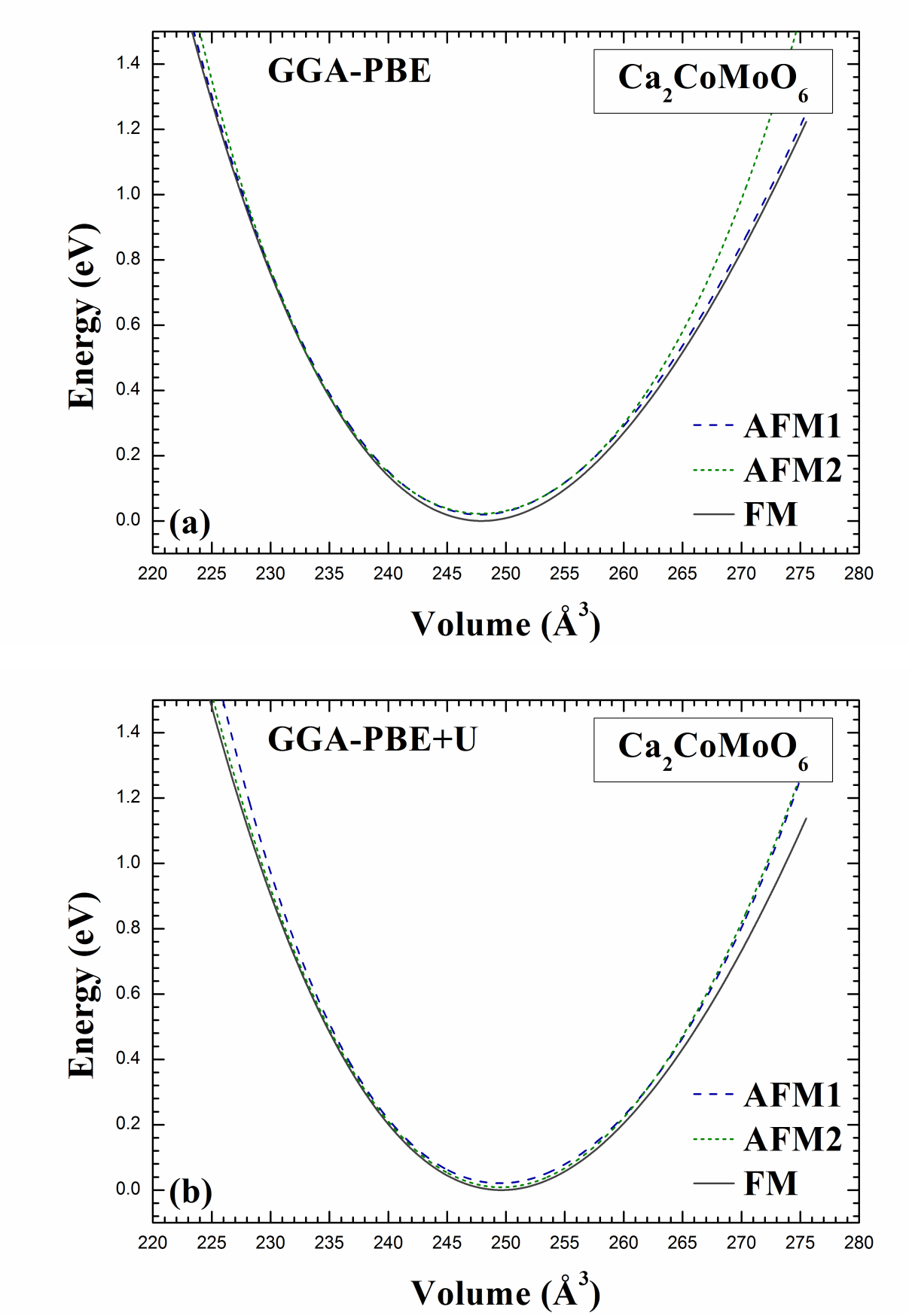
GGA-PBE
Ca2CoMoO6
Energy (eV)
Volume (Å3)
AFM1
AFM2
FM
(a)
GGA-PBE+U
Ca2CoMoO6
Energy (eV)
Volume (Å3)
AFM1
AFM2
FM
(b)

Fig. 4

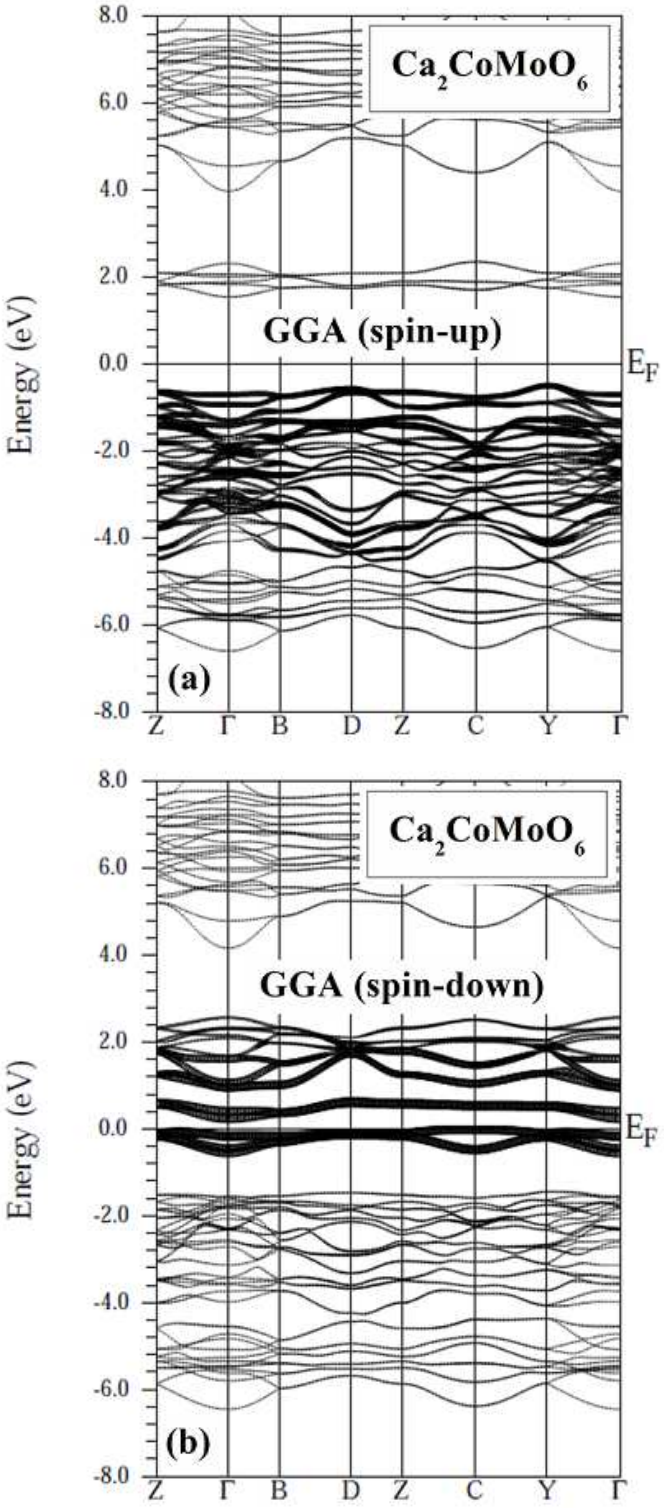
Ca2CoMoO6
GGA (spin-up)
EF
Energy (eV)
8.0
6.0
4.0
2.0
0.0
-2.0
-4.0
-6.0
-8.0
(a)
Z Γ B D Z C Y Γ
Ca2CoMoO6
GGA (spin-down)
EF
Energy (eV)
(b)
Z Γ B D Z C Y Γ

Fig. 5

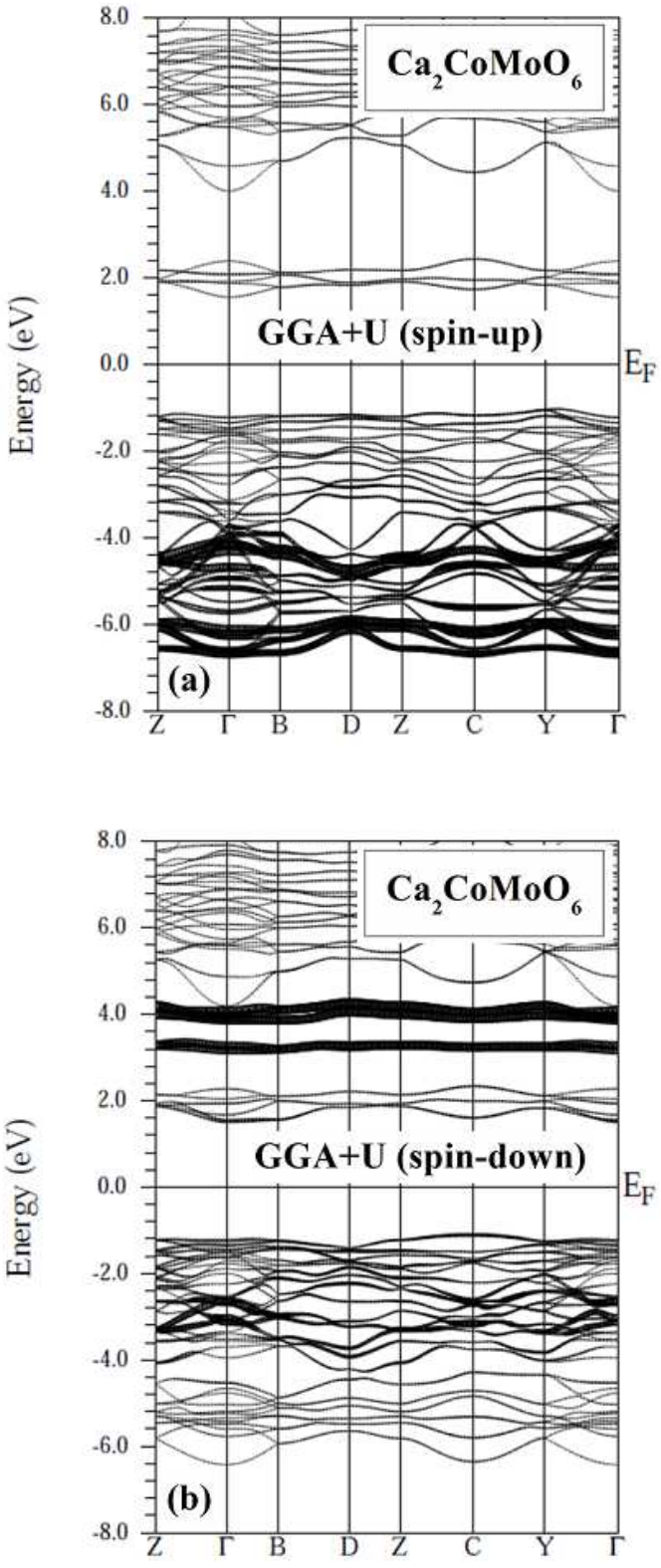
Ca2CoMoO6
GGA+U (spin-up)
Energy (eV)
EF
(a)
8.0
6.0
4.0
2.0
0.0
-2.0
-4.0
-6.0
-8.0
Z Γ B D Z C Y Γ
Ca2CoMoO6
GGA+U (spin-down)
Energy (eV)
EF
(b)
8.0
6.0
4.0
2.0
0.0
-2.0
-4.0
-6.0
-8.0
Z Γ B D Z C Y Γ

Fig. 6

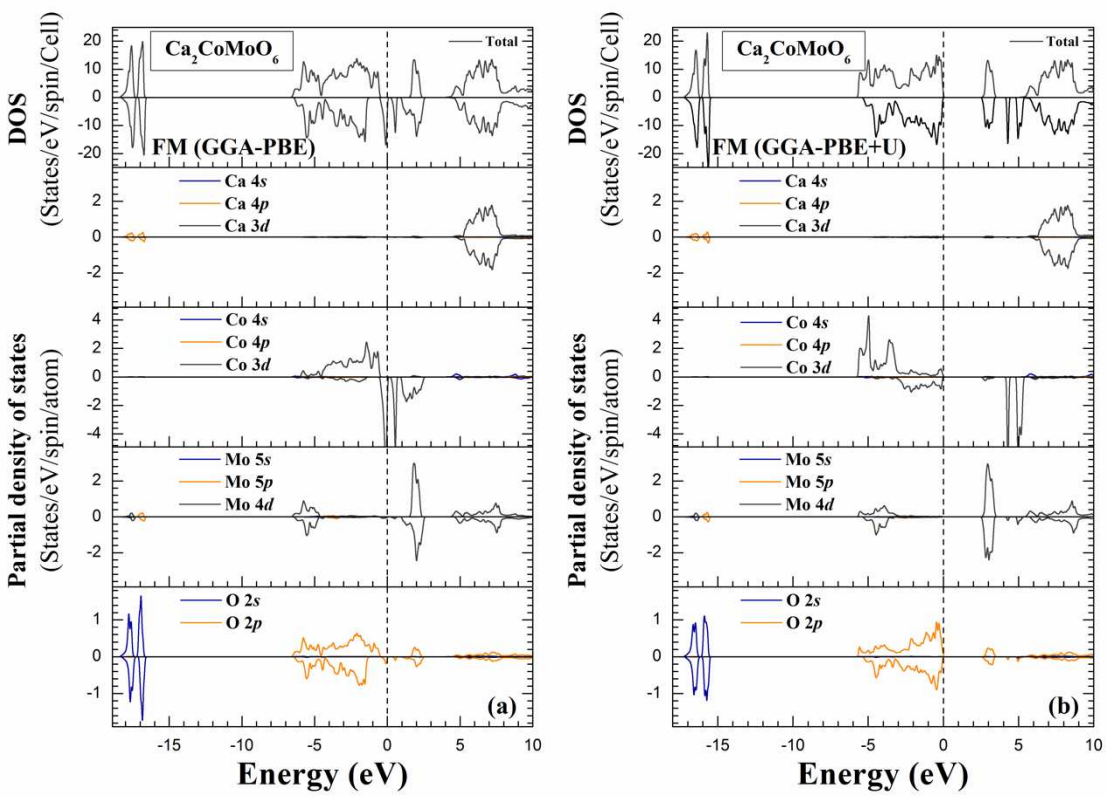
Ca2CoMoO6
FM (GGA-PBE)
FM (GGA-PBE+U)
DOS
(States/eV/spin/Cell)
Partial density of states
(States/eV/spin/atom)
Total
Ca 4s
Ca 4p
Ca 3d
Co 4s
Co 4p
Co 3d
Mo 5s
Mo 5p
Mo 4d
O 2s
O 2p
(a)
(b)
Energy (eV)

Fig. 7

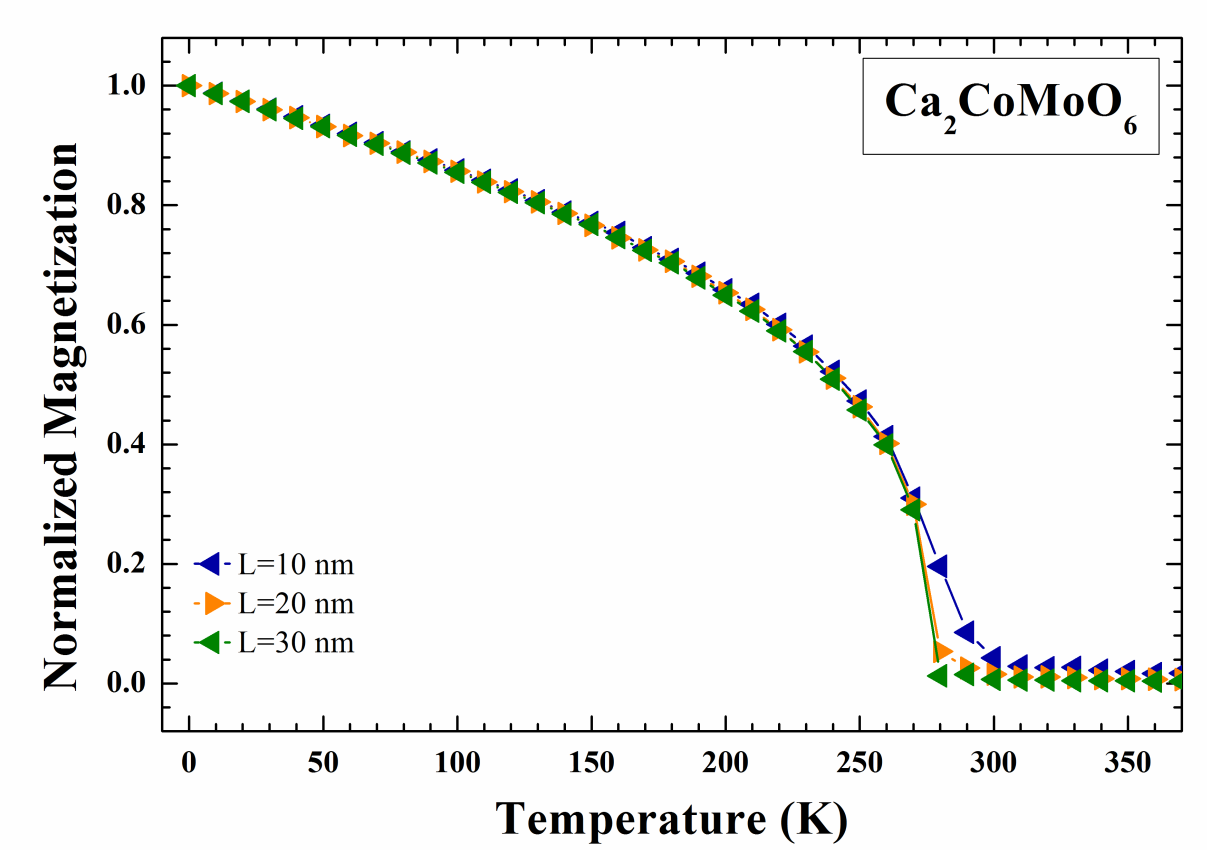
Ca2CoMoO6
Normalized Magnetization
Temperature (K)
L=10 nm
L=20 nm
L=30 nm
0.0
0.2
0.4
0.6
0.8
1.0
0
50
100
150
200
250
300
350

References

[1] K. Schwarz, P. Blaha, G. Madsen, Computer physics communications 147 (2002) 71-76.

[2] Y. Shimakawa, M. Azuma, N. Ichikawa, Materials 4 (2011) 153-168.

[3] A. Maignan, B. Raveau, C. Martin, M. Hervieu, Journal of Solid State Chemistry 144 (1999) 224-227.

[4] N. Moreno, L. Barbosa, D.R. Ardila, J.P. Andreeta, Journal of Superconductivity and Novel Magnetism 26 (2013) 2501-2503.

[5] R. Borges, R. Thomas, C. Cullinan, J. Coey, R. Suryanarayanan, L. Ben-Dor, L. Pinsard-Gaudart, A. Revcolevschi, Journal of Physics: Condensed Matter 11 (1999) L445.

[6] W. Pickett, S. Erwin, E. Ethridge, Physical Review B 58 (1998) 1201.

[7] P. Blaha, K. Schwarz, G. Madsen, D. Kvasnicka, J. Luitz, An Augmented Plane Wave Plus Local Orbitals Program for Calculating Crystal Properties, Vienna University of Technology, Austria, 2012.

[8] C. Bonilla, D. Téllez, J.A. Rodríguez Martínez, J. Roa-Rojas, Brazilian journal of physics 36 (2006) 1101-1104.

[9] D. Sarma, P. Mahadevan, T. Saha-Dasgupta, S. Ray, A. Kumar, Physical Review Letters 85 (2000) 2549.

[10] Z. Szotek, W. Temmerman, A. Svane, L. Petit, H. Winter, Physical Review B 68 (2003) 104411.

[11] K. Momma, F. Izumi, Journal of Applied Crystallography 41 (2008) 653-658.

[12] R.F. Evans, W.J. Fan, P. Chureemart, T.A. Ostler, M.O. Ellis, R.W. Chantrell, Journal of Physics: Condensed Matter 26 (2014) 103202.

[13] R.F. Evans, U. Atxitia, R.W. Chantrell, Physical Review B 91 (2015) 144425.